Liquid droplet dynamics in gravity compensating high magnetic field

V. Bojarevics, S. Easter and K. Pericleous

University of Greenwich, Park Row, London SE10 9LS, UK

Abstract

Numerical models are used to investigate behavior of liquid droplets suspended in high DC magnetic fields of various configurations providing microgravity-like conditions. Using a DC field it is possible to create conditions with laminar viscosity and heat transfer to measure viscosity, surface tension, electrical and thermal conductivities, and heat capacity of a liquid sample. The oscillations in a high DC magnetic field are quite different for an electrically conducting droplet, like liquid silicon or metal. The droplet behavior in a high magnetic field is the subject of investigation in this paper. At the high values of magnetic field some oscillation modes are damped quickly, while others are modified with a considerable shift of the oscillating droplet frequencies and the damping constants from the non-magnetic case.

Introduction

The electromagnetic (EM) and electrostatic levitation experiments with liquid metal droplets show difficulties related to confinement stability and a need for complex correction functions to establish a correlation between the measurements and the droplet material properties [1,2]. Intense internal fluid flow is visually observed, apparently being in the turbulent regime for earthbound conditions. The combination of AC and DC magnetic fields was recently recognized as an efficient tool for the thermo-physical property measurements without a contact to contaminating walls [3,4]. The intense AC magnetic field required to produce levitation results in turbulent large-scale toroidal recirculation within the droplet, which prevents accurate measurements. The use of a homogenous DC magnetic field allows the toroidal flow to be damped. However the turbulence generated in these conditions makes the effective viscosity to behave in a non-linear fashion depending on the DC and AC magnetic field intensity [4]. The flow in a typical droplet is approaching the conditions with laminar viscosity and heat transfer when a uniform DC magnetic field exceeds about 4-5 T. For even higher DC magnetic field the levitation, using para- and dia-magnetic properties of the materials, can be used for advanced material research [5,6]. The vertical field gradient permits to compensate gravity along the central axis, while the radial variation acts to centre it on the axis for stable levitation. In practice a small vibration of the droplet as a whole remains even in carefully conducted experiments [6]. Frequency measurements using the oscillating drop technique have been conducted for water droplets by Beaugnon et al. [5], where estimates were made as to the frequency modification due to the magnetic field. More recent experiments have been conducted by Hill & Eaves [6], in which a derivation of the frequency modifications due to the magnetic field are made and compared with the experimental results.

The oscillations in a high DC magnetic field are quite different for an electrically conducting droplet. In a recent publication [7] an asymptotic solution for very high magnetic field shows damping of the even axisymmetric modes, but the odd modes are not damped or damped

moderately. The asymptotic linear theory predicts a considerable shift of the oscillating droplet frequencies from the non-magnetic case. The droplet behavior in high magnetic field is the subject of investigation in this paper. Numerical models of the flow coupled with the moving free surface give an insight to the dynamics of levitated droplets of various sizes and magnetic field intensities. The realistic gradient fields, as in the solenoidal coils of superconducting magnets, are used for the modeling experiments with electrically non-conducting (water) and conducting (liquid silicon) droplets.

Droplet oscillation numerical model

The free surface shape of the droplet is defined by a deviation from a sphere of radius R_0. The surface position can be represented in the spherical co-ordinates by a function S of time and the angular coordinates:

$$r_s = R_0 \left[1 + S(\theta, \phi, t) \right].$$
(1)

The mode dependent oscillation frequency and damping constants are generally derived by following a perturbation approach. The S function can be represented as a series of spherical harmonics:

$$S(\theta, \phi, t) = \sum_{L=0}^{L=\infty} \sum_{M=0}^{M=L} A_L^M(t) P_L^M(\cos\theta) e^{iM\phi}.$$
(2)

The $Y_0^0 = P_0^0$ mode is included to account for conservation of mass (volume) of the sphere with radius R_0 if an initial perturbation of the surface is given. The time-dependent surface coefficients are assumed to be harmonic with exponential damping:

$$A_L^M(t) = e^{(i\omega_L^M - \gamma_L^M)t}.$$
(3)

The zero order (in powers of the perturbation amplitude) result for the frequency was obtained by Rayleigh, and is given for a droplet with density ρ and surface tension Γ by:

$$\omega_L^M = \sqrt{L(L-1)(L+2)\Gamma / (\rho R_0^3)}.$$
(4)

The damping coefficient for a droplet of viscosity ν was determined by Lamb:

$$\gamma_L^M = (L-1)(2L+1)\nu / R_0^2.$$
(5)

The zero order approximation for both the frequency and the damping constant are independent of the azimuthal number M. These formulae provide a good first approximation for low amplitude oscillations of droplets in microgravity conditions where the effects of any external forces used to position the droplet are negligible compared with surface tension and viscous forces. However it is worth noting that these formulae are restricted and are only valid in the limit that the amplitude of oscillation and also non-linear effects tend to zero. Modifications to these have been derived by Tsamopoulos & Brown [8] for 'moderate amplitude': the frequency decreases with increasing amplitude and a coupling of modes appears at the second order.

In a recent paper Priede [7], considers the effect of a constant high intensity magnetic field on the oscillation frequency and damping rate of an electrically conducting drop. The magnetic field is shown to significantly alter the dynamics of the droplet with some interesting results. There are two distinct cases: the longitudinal modes when (L-M) is odd and the transversal modes when (L-M) is even. The frequencies for the odd modes including the axisymmetric (M=0, of the greatest interest for this paper) are given by:

$$\omega_L^M = \sqrt{(L-1)(L+2)\Gamma / (\rho R_0^3)},$$
(6)

which is √L less than the normal mode frequencies (4). In the following section an outline is given of an axisymmetric and a 3D numerical model that will be used to investigate these effects. Following results are presented that demonstrate quantitatively the theoretical predictions and the

deviations from the zero order asymptotic theory due to the presence of the gravity field and finite amplitude oscillations.

The numerical model uses a grid point formulation of the spectral collocation method [10] with the Chebyshev grid for the radial direction and Fourier in the angular directions. The model uses a coordinate transformation for the free surface, which allows the problem to be solved on a unit sphere. The equations solved by the numerical model are the momentum and mass conservation equations with the modified pressure, $P_{mod} = P + \rho g R \cos\theta - \chi_v |B|^2 / (2\mu_0)$:

$$\partial_t \mathbf{V} + (\mathbf{V}\cdot\nabla)\mathbf{V} = -\rho^{-1}\nabla P_{mod} + \nu\nabla\cdot(\nabla\mathbf{V} + \nabla\mathbf{V}^T) + \rho^{-1}\mathbf{J}\times\mathbf{B}; \quad \nabla\cdot\mathbf{V} = 0. \tag{7}$$

The total force due to the magnetic field consists of two components, the Lorentz force due to the conducting properties, which is added to the momentum equations as a body force and the diamagnetic force, which is potential and is implemented in the model as boundary condition to the pressure equation along with the gravitational force, which is also potential. The full boundary conditions for the equations (7) relate the normal stress to the surface tension:

$$\mathbf{e_n} \cdot \Pi \cdot \mathbf{e_n} = \Gamma K, \tag{8}$$

continuity of the velocity field and the tangential stress conditions:

$$\nabla\cdot\mathbf{V} = 0, \quad \mathbf{e_n}\cdot\Pi\cdot\mathbf{e}_{\tau 1} = 0, \quad \mathbf{e_n}\cdot\Pi\cdot\mathbf{e}_{\tau 2} = 0, \tag{9}$$

where $\mathbf{e}_n, \mathbf{e}_{\tau 1}, \mathbf{e}_{\tau 2}$ are the unit vectors normal and tangential to the free surface, Π is the stress tensor, K is the surface curvature, and χ_v is the volumetric magnetic susceptibility. The free surface shape given by (1) is updated at each time step using the kinematic condition:

$$\partial_t \mathbf{r}_s \cdot \mathbf{e_n} = \mathbf{V}\cdot\mathbf{e_n}. \tag{10}$$

The magnetic field in a solenoid is modelled as a superposition of the magnetic field generated by axisymmetric coil filaments of finite cross-section (see Figure 1 as an example). The axisymmetric magnetic field is obtained from the analytical formulae [9].

The stable levitation conditions can be established by adjusting the electric current in the coils to form a minimum in the magneto-gravitational potential:

$$U = g R \cos\theta - \chi_v |\mathbf{B}|^2 / (2\rho\mu_0). \tag{11}$$

The electromagnetic body force requires in general an additional equation to be solved for the electric potential (only in the 3D case). The electric current density is given by:

$$\mathbf{J} = \sigma(-\nabla\phi_E + V\times\mathbf{B}). \tag{12}$$

The equation for the electric potential is obtained from the charge conservation $\nabla\cdot\mathbf{J} = 0$. Taking the divergence of the electric current density gives:

$$\nabla^2\phi_E = \nabla\cdot(V\times\mathbf{B}). \tag{13}$$

This equation is solved subject to the condition at the instantaneous drop surface: $\mathbf{J}\cdot\mathbf{e}_n = 0$.

Results & Discussion

The following section contains the results of numerical simulations made using both the 2D axisymmetric [10] and 3D modes compared with experimental results [6] and theoretical asymptotic results [7]. The material chosen for the numerical test cases is either water (diamagnetic, electrically non-conducting) or molten silicon (diamagnetic, electrically conducting) having the material property values given in the Table 1.

Symbol	Quantity	Water	Silicon	Units
Γ	Surface Tension Coefficient	0.0733	0.865	N m^{-1}
ρ	Density	999.0	2510.	Kg m^{-3}
ν	Kinematic Viscosity	1.11e-6	1.0e-6	m^2 s^{-1}
χ_v	Volumetric Magnetic Susceptibility	-9.0e-6	-4.2e-6	N/A

Table 1. The material property values used for the numerical test cases.

The numerical simulation uses the superposition of the modes L = 2,3,4,5,6,7 for axisymmetric surface shape, or L=2, M=1 for the 3d test as the initial condition. The amplitude coefficient is chosen to give a deformation of 1% of the unperturbed radius (R_0 = 5mm or 10 mm). A spherically symmetric constant component (L=0) is also required to ensure the initial surface shape conserves the mass of the droplet based on the equilibrium spherical radius.
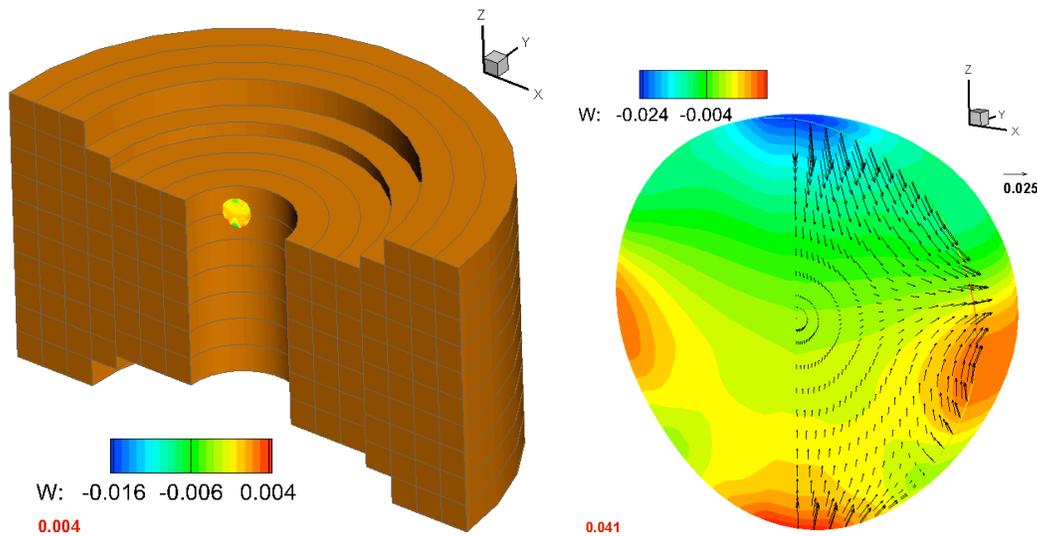
Figure 1. Water droplet R_0 = 10 mm in the bore of solenoid magnet and the initial velocity field (color contours for vertical velocity component W and the scale vector in m/s).

Water Droplet in Solenoid Magnet

Figure 1 shows the droplet in the solenoid magnet and the zoom-in view to the initial velocity field after 41 ms, generated by the axisymmetric surface deformation condition in the simulation. The droplet is positioned in the upper part of the magnet 8 cm above the magnet centre. We attempted to preserve dimensions similar to the experiment [6], however the exact design of the magnet is a proprietary information not available for this modelling work. The magnetic field and the required magneto-gravitational potential (11) are updated at each time step of maximum length 0.000125s. The instantaneous distributions of the magnetic field are computed only in the volume occupied by the droplet as shown in the Figure 2. The magnetic field at the top part of the solenoid is reduced in magnitude relative to the central part where it is about 16.5 T.
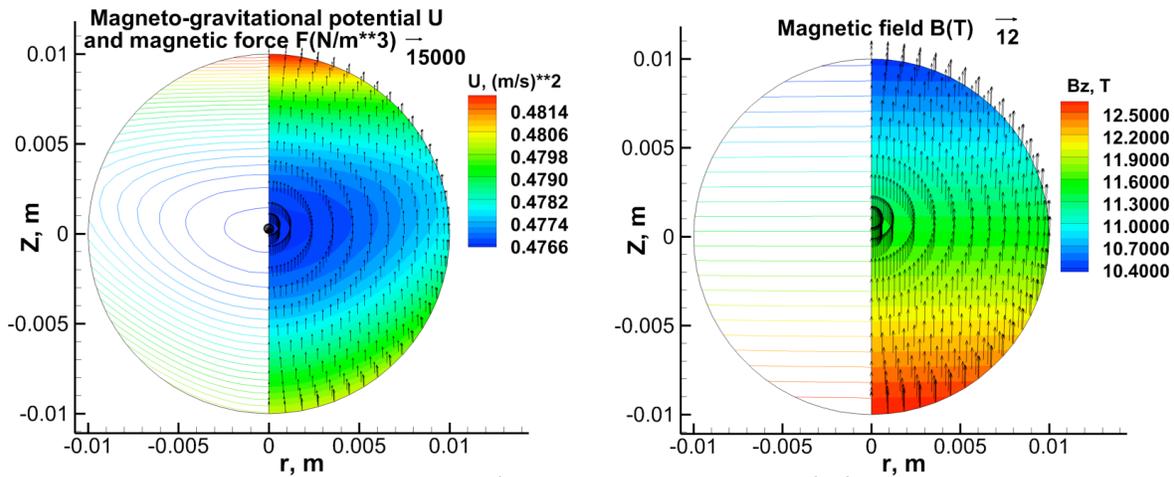
Figure 2. Magnetic field in T, force (N/m^3) and the potential U (m^2/s^2) in the water droplet R$_0$ = 10 mm at the top part of the solenoid magnet. (The reference vector scales in respective units.)
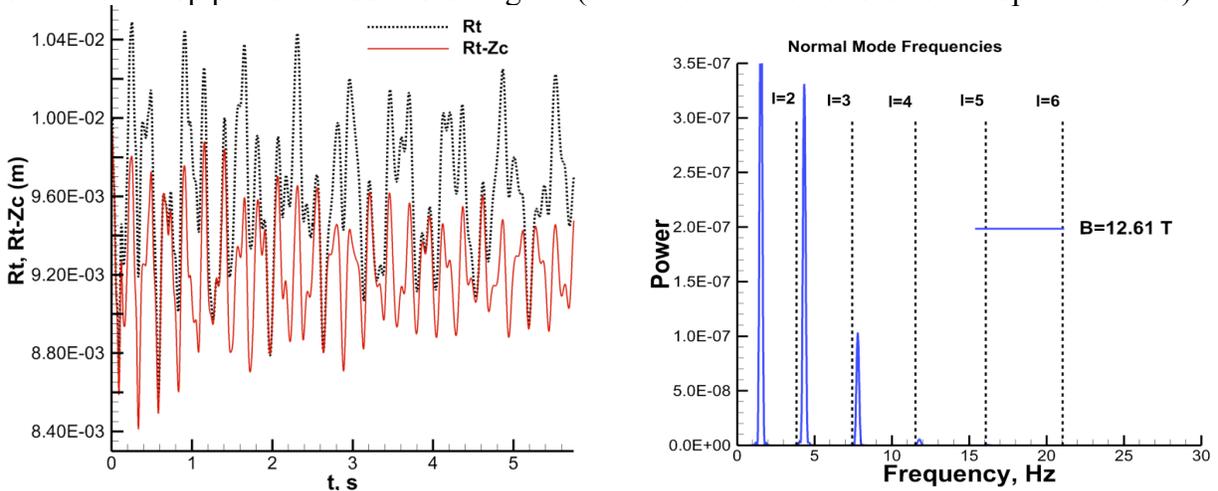
Figure 3. Oscillations of the surface top position Rt and Rt-Zc (difference to centre of mass position), and power (relative units) spectra computed for water droplet R$_0$ = 10 mm.

The computed oscillation pattern appears to be of similar nature as observed in the experiments [6], i.e., the frequency spectra peaks are slightly shifted to increase the mode frequencies relative to the non-magnetic Rayleigh values (4). The oscillation pattern shown in the Figure 3 indicates a considerable centre of mass position influence on the surface variation. The droplet position as a whole vibrates with a very small amplitude, typically less than 1 mm [6]. The numerical results in the Figure 3 give the oscillation of the surface top position difference to the centre of mass position: Rt-Zc (t). This function clearly shows the decay of the surface oscillation, while the Zc continues to move without an apparent damping.

Figure 4 illustrates the centre of mass oscillation for a smaller size water droplet R$_0$ = 5 mm. In this numerical run we additionally modified the electric current in the solenoid so that the droplet is stably levitated in a region of higher magnetic field (max B = 15.46 T). In this case the centre of mass oscillates with a small amplitude of about 0.01 mm. The surface oscillation is damped at different rate for various amplitudes, apparently the mode L = 3 is the dominant as the power spectra for this case shows (Figure 4). The other remarkable feature for this case is the systematic reduction of all the frequencies relative to the non-magnetic values (4) and contrary to the observations in [6]. The explanation for this discrepancy is the effect of the finite amplitude shifting the frequency to smaller values [8] as supported by our tests running the same simulation with B = 0 (not shown due to space restrictions).
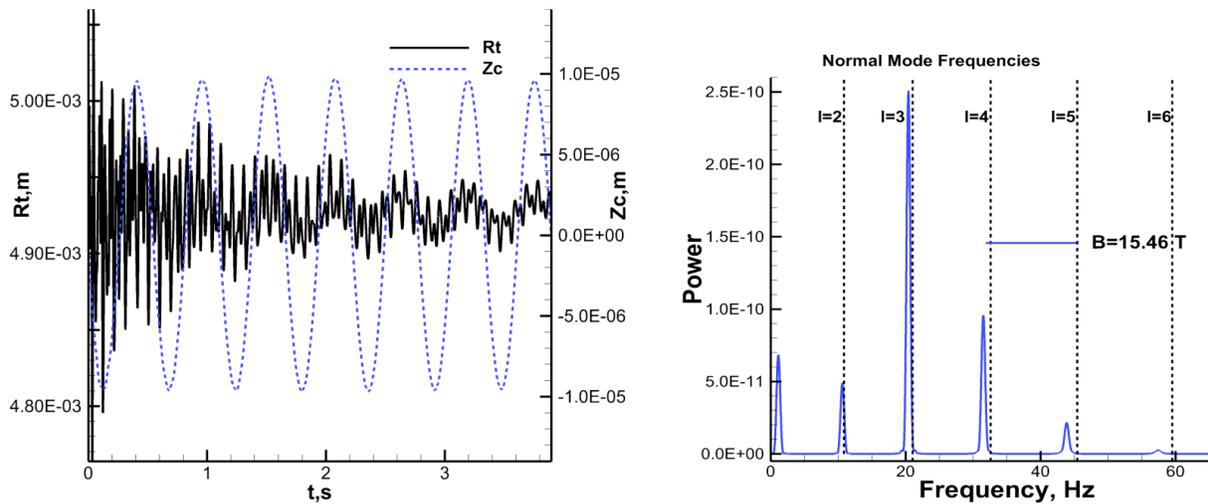
Figure 4. Oscillations of the surface top Rt and the centre of mass Zc, and Rt power spectra (in relative units) computed for the water droplet $R_0 = 5$ mm.

3d Water Droplet Oscillations in Solenoid Magnet

A 3d test case generally supports the more accurate axisymmetric simulations. A numerical procedure is used to analyze the surface shape at each time-step in order to determine the relative contribution of each mode. This results in time dependent coefficient for each of the spherical harmonic modes. The dominant components are the $L = 2$, $M = 1$ mode, which corresponds to the initial condition, axisymmetric modes $L = 2$, $M = 0$, and $L = 3$, $M = 0$, which are introduced by the external forces, and the $L = 1$, $M = 0$ translational mode. Other small components are also present that ensure the conservation of mass. Figure 5 shows the computed instantaneous 3d velocity field and the oscillations corresponding to the dominant mode with the respective power spectra. The theoretical value for the normal mode, derived for the magnetic modification to the first order [6], is indicated in the power spectra with dashed line.
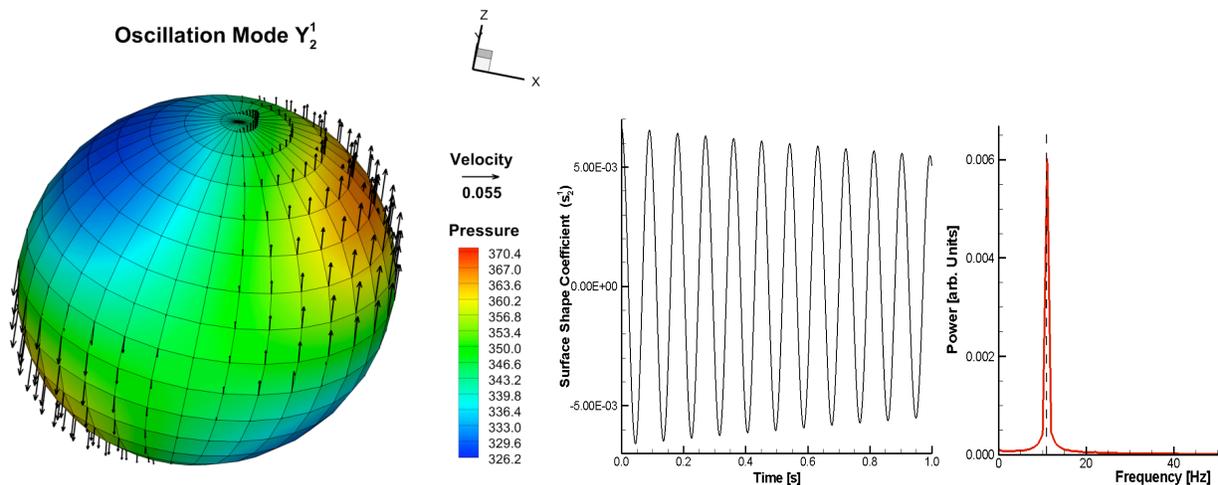
Figure 5. The 3d instantaneous velocity and pressure on the surface, and the oscillations of the top with the power spectra computed for the water droplet $R_0 = 5$ mm.

Table 2 compares the theoretical frequencies and the frequencies calculated numerically. There is a reasonable agreement between the theoretical and numerical values. The frequency shifts are small, but not insignificant when considered in the context of surface tension measurements.

68

	Y^0_1	Y^0_2	Y^1_2	Y^0_3
Normal Mode, see (4)	N/A	1.09e+1	1.09e+1	2.11+1
Theoretical [6]	N/A	1.12e+1	1.11e+1	2.14e+1
Numerical	1.62e+0	1.11e+1	1.11e+1	2.13e+1

Table 2. The frequency calculations for 3d water droplet oscillations.

Liquid Silicon Droplet in Solenoid Magnet

An electrically conducting levitated droplet motions are expected to be damped in strong DC magnetic field, however some types of movement are not affected in a particular field configurations. In the microgravity case (g = 0) and a uniform vertical magnetic field the asymptotic solution [7] shows that odd axisymmetric oscillation modes are very moderately damped and the frequencies are reduced by a factor of √L (6). It is not immediately clear if this behavior will stay in the presence of terrestrial gravity and the gradient magnetic field required for the magnetic levitation. The numerical experiments with liquid silicon appear to support the general conclusions of the asymptotic solution as demonstrated by the Figure 6. The L = 3 (see the velocity field in the Figure 7) and the longitudinal centre of mass L = 0 modes are the only ones not damped immediately in the 17 T magnetic field required to levitate the 5 mm radius liquid silicone droplet. The frequency of the L = 3 mode is reduced about √3 times relative to the non-magnetic case (4) and closely matches the theoretical value [7]. The small deviation can be explained by the presence of the gradient part of the magnetic field. By readjusting the electric current in the solenoid the gradient part can be reduced at the expense of increased uniform B_z component. When the magnitude of the field is 28 T the computed frequency is practically coinciding with the theoretical value to the accuracy of 0.01%. However in this case the droplet weight is balanced only at the initial time, then vigorous oscillations of the modes L = 3 and L = 1 (centre of mass) follow (Figure 7), and the droplet very slowly slides downwards (Figure 8). The magneto-gravitational potential on the surface $U(R = r_s) = \sum_{n=0} U_n(t) P_n(\cos\theta)$ experiences similar oscillations to the free surface shape as shown in the Figure 8.
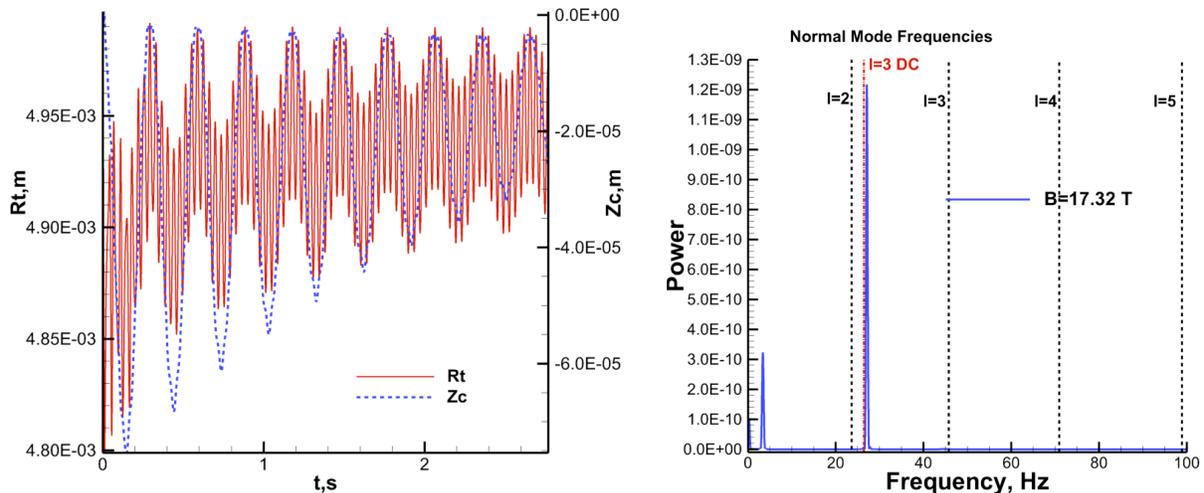
Figure 6. Oscillations of the surface Rt and the centre of mass Zc, and Rt power spectra computed for the liquid silicon droplet $R_0 = 5$ mm in 17 T field.
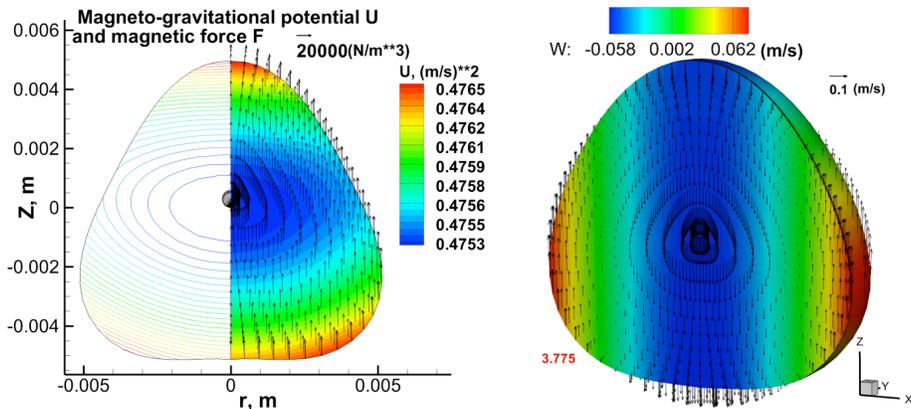
Figure 7. Magnetic potential, force and velocity field in the liquid silicon droplet $R_0 = 5$ mm.
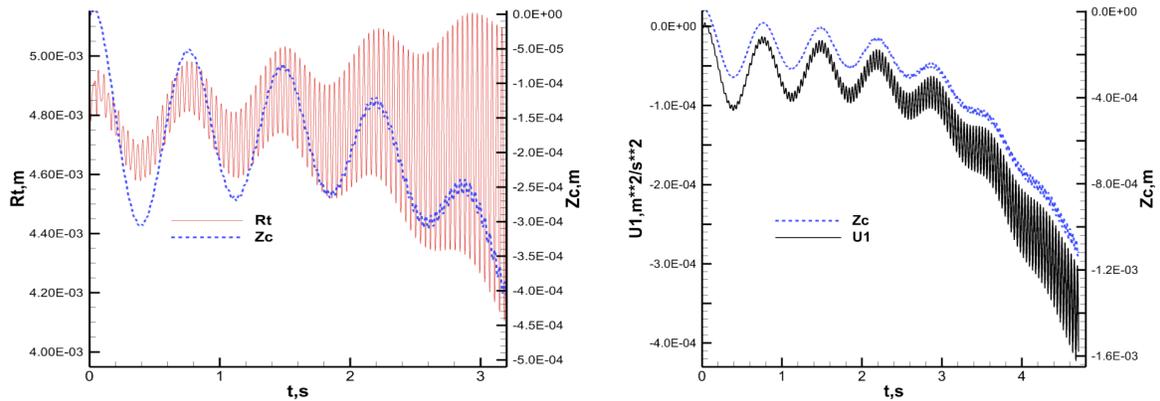
Figure 8. Oscillations of the surface Rt, centre of mass Zc, and the magnetogravitational potential expansion linear coefficient U_1 for the liquid silicon droplet $R_0 = 5$ mm in 28 T field.

References

[1]   Egry I, Lohofer G, Seyhan I, Schneider S and Feuerbacher B 1999 "Viscosity and surface tension measurements in microgravity" Int. J. Thermophys. 20 (4) 1005-1015

[2]   Cummings D L and Blackburn D A 1991 "Oscillations of magnetically levitated aspherical droplets" J. Fluid Mech. 224 395-416

[3]   Kobatake H, Fukuyama H, Minato I, Tsukada T and Avaji S 2007 "Noncontact measurement of thermal conductivity of liquid silicon in a static magnetic field" Applied Physics Letters 90 094102

[4]   Bojarevics V, Easter S, Roy A and Pericleous K 2009 "Levitated Liquid Droplets in AC and DC Magnetic Field" Proc. Int. Symp.Liquid Metal Processing and Casting, Santa Fe, TMS, ed-s Lee P, Mitchell A, Williamson R, 319-326

[5]   Beaugnon E, Fabregue D, Billy D, Nappa J and Tournier R 2001 "Dynamics of magnetically levitated droplets" Physica B 294-295 715-720

[6]   Hill R J A and Eaves L 2010 "Vibrations of a diamagnetically levitated water droplet" Phys. Rev E 81 (5) 056312

[7]   Priede J 2010 "Oscillations of weakly viscous conducting liquid drops in a strong magnetic field" J. Fluid Mech. 671 399-416

[8]   Tsamopoulos J A and Brown R A 1983 "Nonlinear oscillations of inviscid drops and bubbles" J. Fluid Mech. 127 519-537

[9]   Smythe W R 1950, Static and Dynamic Electricity, McGraw-Hill, London

[10]   Bojarevics V and Pericleous K 2003 "Modelling electromagnetically levitated liquid droplet oscillations" ISIJ International 43 (6) 890-898